



Dalton
Transactions

Theoretical Rationalization for the Equilibrium between (μ - $\eta^2:\eta^2$ -Peroxido) $\text{Cu}^{\text{II}}\text{Cu}^{\text{II}}$ and Bis(μ -oxido) $\text{Cu}^{\text{III}}\text{Cu}^{\text{III}}$ Complexes: Perturbational Effects from Ligand Frameworks

Journal:	<i>Dalton Transactions</i>
Manuscript ID	DT-ART-03-2020-001001.R1
Article Type:	Paper
Date Submitted by the Author:	14-Apr-2020
Complete List of Authors:	Abe, Tsukasa; Kyushu University Shiota, Yoshihito; Kyushu University Itoh, Shinobu; Osaka University Yoshizawa, Kazunari; Kyushu University

SCHOLARONE™
Manuscripts

ARTICLE

Theoretical Rationalization for the Equilibrium between (μ - η^2 : η^2 -Peroxido)Cu^{II}Cu^{II} and Bis(μ -oxido)Cu^{III}Cu^{III} Complexes: Perturbational Effects from Ligand Frameworks

Received 00th January 20xx,
Accepted 00th January 20xx

DOI: 10.1039/x0xx00000x

Tsukasa Abe,^a Yoshihito Shiota,^a Shinobu Itoh^b and Kazunari Yoshizawa*^a

DFT calculations are carried out to investigate the geometric effects of the supporting ligands in the relative energies of the (μ - η^2 : η^2 -peroxido)Cu^{II}Cu^{II} complex **1** and the bis(μ -oxido)Cu^{III}Cu^{III} complex **2**. The N₃-tridentate ligand bearing acyclic propane diamine framework **La** preferentially provided **1**, whereas the N₃-tridentate ligand with cyclic diamine framework such as 1,4-diazacycloheptane **Lb** gave **2** after the oxygenation of the corresponding Cu^I complexes as reported previously [S. Itoh, *et al Inorg. Chem.*, 2014, **53**, 8786–8794]. Calculations at the B3LYP*-D3 level of theory can reasonably explain the experimental results in relative energies, structures and harmonic frequencies of **1** and **2**. Perturbational effects of the diamine chelates of **La** and **Lb** especially on the equilibrium of **1** and **2** are investigated in detail. In the range from 2.30 Å to 3.40 Å of the N–N distance in the diamine moiety, **1** is more stable than **2** by 8.4 kcal/mol at the distance of 3.40 Å. Calculated potential energies indicate that the decrease in the N–N distance is associated with a decrease in energy of **2**, leading that **2** can be most stabilized at the N–N distance of 2.60 Å. Furthermore, molecular orbitals analyses are performed to explain that the energy gaps between the σ^* orbital of the O–O bond and the $d_{x^2-y^2}$ orbitals of the Cu^{II} ions of **1** get small as the diamine moiety is shrunk, leading to facilitate the O–O bond cleavage from **1** to **2**.

Introduction

Dicopper-dioxygen adducts have attracted much recent attention due to their importance as models for Type 3 copper proteins that participate in O₂-binding and activation.^{1–7} For example, hemocyanins are well-known oxygen carrier proteins in arthropods and mollusks. Tyrosinases catalyze the oxygenation of phenols to catechols and further oxidation of catechols to *ortho*-quinones, whereas catechol oxidases are responsible only for the conversion of catechols to *ortho*-quinones.⁸ The oxy-forms of these proteins have been shown by X-ray crystallography to involve a μ - η^2 : η^2 -peroxo binding mode.^{9–11} The main text of the article should appear here with headings as appropriate.

In the synthetic modeling studies, Kitajima and co-workers have successfully obtained the first crystal structure of the (μ - η^2 : η^2 -peroxido)Cu^{II}Cu^{II} complex **1** (Fig. 1), which was generated

via the reduction of O₂ by two copper(I) complexes as a model for the active sites of the oxy-forms of hemocyanin, tyrosinase and catechol oxidase.^{12–14} In certain ligand systems, further two-electron reduction of the peroxide moiety takes place to induce O–O bond homolytic cleavage to give the bis(μ -oxido)Cu^{III}Cu^{III} complex **2** (also in Fig. 1), which was first structurally characterized by Tolman and co-workers.^{15–17} Even though **2** has yet to be observed in any enzymatic reactions, it has been considered to be formed as a transient reactive intermediate^{18,19} because the interconversion between **1** and **2** has been shown to exhibit a low activation energy barrier.^{1,7,20} It has been well established in the synthetic modeling studies that the equilibrium between **1** and **2** can be controlled by electronic-, geometric- and steric effects of the supporting ligands^{3,21–37} as well as the polarity of solvents^{38–40} and the basicity of counter anions.^{41,42}



Fig. 1 Core structures of dicopper-dioxygen complexes.

Along with the synthetic modeling studies mentioned above, theoretical studies have been carried out to investigate the electronic structures of **1** and **2** and the mechanism of the O–O bond cleavage in **1** giving **2**.^{43–71} The energy difference between the two forms strongly depends on functionals and basis sets used. Pierloot and co-workers indicated that the equilibrium is

^a Institute for Materials Chemistry and Engineering and IRCCS, Kyushu University, 744 Motoooka, Nishi-ku, Fukuoka, Japan. E-mail: kazunari@ms.ifoc.kyushu-u.ac.jp

^b Department of Material and Life Science, Division of Advanced Science and Biotechnology, Graduate School of Engineering, Osaka University, 2-1 Yamadaoka, Suita, Osaka, Japan

† Electronic Supplementary Information (ESI) available: Fig. S1: Plots of the energy differences between **1** and **2** along with the ratio of the Hartree–Fock exchange in the functionals; Fig. S2: Calculated energy differences between **1** and **2** without Grimme's dispersion correction (D3); Fig. S3: Schematic representations and Walsh diagram in **1a**; Fig. S4: Plots of energy gaps between the σ^* and $d_{x^2-y^2}$ orbitals in **1a**; Fig. S5: Plots of the O1–O2 bond distance in **1a**; Fig. S6: Plots of Mayer bond order of the O1–O2 bond in **1a**; Fig. S7: Plots of energy gaps between the $d_{x^2-y^2} - \sigma^*$ and $d_{x^2-y^2} + \sigma^*$ orbitals in **2a**; Table S1–S4: Cartesian coordinates of **1a**, **2a**, **1b** and **2b**. See DOI: 10.1039/x0xx00000x

shifted towards **2** by relativistic effects.⁵⁵ The same strategy was followed later by Rode and Werner.⁶⁵ Cramer and co-workers indicated that the incorporation of the Hartree–Fock exchange in hybrid density functionals was found to have a significant effect on the prediction of the relative energy between **1** and **2**.⁶⁶ According to their report, **1** is stabilized in energy by 5–10 kcal/mol when the ratio of the Hartree–Fock exchange is increased by 10%. Recently, Witte and Herres-Pawlis⁷¹ rationalized the effects at the chemical level by finding relativistic bond stabilization in **1** and **2**. In addition, the lack of dispersion corrections also favors **1** compared to **2**. Liakos and Neese pointed out that only at the highest level of theory involving complete basis set extrapolation, triple excitation contributions as well as relativistic and solvent effects, **2** is found to be slightly more stable than **1**.⁶⁷ They also found that **2** is more stable than **1** using the B3LYP functional with dispersion corrections.

Previously, Abe, Itoh and co-workers reported that a subtle ligand modification greatly impacts the reactivity of Cu(I) complexes toward molecular oxygen.³⁶ As shown in Fig. 2, ligand **La** having acyclic diamine framework affords **1** as a major product together with **2** as a minor product, whereas analogous ligand **Lb** having a 7-membered cyclic diamine framework provides only **2** in the oxygenation reaction of the copper(I) complexes at –85 °C in acetone. Despite the same donor sets in **La** and **Lb** (one-pyridine nitrogen and two alkylamine nitrogens), the N2–N3 distances of **La** are significantly changed depending on the oxidation states of the copper ions. Namely, the N2–N3 distances are 3.298 Å in the copper(I) complex of [Cu^I(**La**)](PF₆) and 3.067 Å in the copper(II) complex of [Cu^{II}(**La**)(Cl)](PF₆).³⁶ On the contrary, the N2–N3 distances of **Lb** are much shorter than those in the **La** ligand system and hardly changed both in the copper(I) and copper(II) oxidation states; the N2–N3 distances are 2.678 Å in the copper(I) complex [Cu^I(**Lb**)](PF₆) and 2.613 Å in the copper(II) complex [Cu^{II}(**Lb**)(Cl)₂].³⁶ These structural effects may contribute to the reactivity difference of the copper(I) complexes of **La** and **Lb** toward molecular oxygen, as mentioned above.

In this work, we set up and calculated four kinds of dicopper-dioxygen complexes **1** and **2** supported by **La** and **Lb** consisting with the acyclic and cyclic diamine frameworks, respectively. Then, we investigated how the N2–N3 distance of the diamine framework controls the equilibrium between **1** and **2** using DFT calculations and molecular orbital analyses.

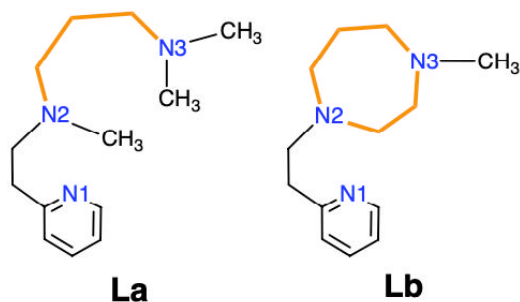


Fig. 2 N₃-tridentate ligands consisting with acyclic-diamine framework **La** and cyclic-diamine framework **Lb**.

Computational methods

The B3LYP method⁷² has been widely used for the simulation of various transition-metal complexes for more than 25 years. However, it tends to overestimate the stability of the (μ - η^2 : η^2 -peroxido)Cu^ICu^{II} complexes compared to that of the bis(μ -oxido)Cu^{III}Cu^{III} complexes. We also confirmed this general tendency, as shown in Fig. S1 of the ESI. To avoid this problem, we used a newly parametrized version of B3LYP developed by Reiher and co-workers:⁷³ the B3LYP* functional with 15% Hartree–Fock exchange instead of 20% in the B3LYP functional. All calculations were performed by using the spin-unrestricted DFT (UDFT) implemented in the Gaussian 16 package⁷⁴ for structural optimizations. We used the (16s10p6d) primitive set of Wachters–Hay supplemented with one polarization f-function ($\alpha = 1.44$ for Cu)⁷⁵ for the Cu atoms and the D95** basis set for the H, C, N and O atoms.⁷⁶ We added Grimme’s dispersion correction (D3)⁷⁷ because Liakos and Neese suggested that Grimme’s dispersion correction gave a very good guess for the energies of **1** and **2**.⁶⁷ Without this correction, the prediction of the energies of **1** and **2** is not appropriate, as shown in Fig. S2 of the ESI. Therefore, we used the D3 parameters for the B3LYP functional. Siegbahn and co-workers reported that the energies of some metalloenzyme active sites calculated by B3LYP*-D3 are almost identical to those calculated by B3LYP-D3.⁷⁸ For the calculations of the (μ - η^2 : η^2 -peroxido)Cu^ICu^{II} complexes, we initially adopted triplet state ($S = 1$) and then computed open-shell singlet (OSS) energies using the broken-symmetry approach. After structural optimizations, vibrational analyses were performed to ensure that no imaginary frequencies were found. Cramer and co-workers indicated that the continuum solvation calculations predict electrostatic effects to favor the bis(μ -oxo)Cu^{III}Cu^{III} complexes over the (μ - η^2 : η^2 -peroxido)Cu^ICu^{II} complexes by 1–4 kcal/mol.⁶⁶ Because we consider the effects of the solvation required for the prediction of the relative energy between **1** and **2**, implicit solvent effects were included by using the polarized continuum model (PCM).⁷⁹ In this work, the N₃-substituent of **Lb** was replaced to the methyl group (–CH₃) instead of the phenethyl group (–CH₂CH₂C₆H₅) used in the experimental studies by Abe and Itoh et al.³⁶ to exclude effects of the ligand sidearm.

Results and discussions

Energies, Frequencies and Structures. Fig. 3 shows calculated energies of the (μ - η^2 : η^2 -peroxido)Cu^ICu^{II} (**1a** and **1b**) and the bis(μ -oxido)Cu^{III}Cu^{III} (**2a** and **2b**) complexes generated by using ligands **La** and **Lb** at the B3LYP*-D3 level of theory. The (μ - η^2 : η^2 -peroxido)Cu^ICu^{II} complex, [Cu^I₂(**La**)₂(O₂²⁻)₂]²⁺ (**1a**), is more stable than the bis(μ -oxido)Cu^{III}Cu^{III} complex, [Cu^{III}₂(**La**)₂(O₂²⁻)₂]²⁺ (**2a**), in the **La** ligand systems by 4.1 kcal/mol, whereas the bis(μ -oxido)Cu^{III}Cu^{III} complex, [Cu^{III}₂(**Lb**)₂(O₂²⁻)₂]²⁺ (**2b**), is more stable than the (μ - η^2 : η^2 -peroxido)Cu^ICu^{II} complex, [Cu^I₂(**Lb**)₂(O₂²⁻)₂]²⁺ (**1b**), by 6.9 kcal/mol in the **Lb** ligand systems.

These results are consistent with the experimental results in that **La** provided the the (μ - η^2 : η^2 -peroxido)Cu^ICu^{II} complex as a major product together with the corresponding bis(μ -oxido)Cu^{III}Cu^{III}

complex as a minor product, whereas **Lb** analogue gave the bis(μ -oxido)Cu^{III}Cu^{III} complex as the solely detectable product.³⁶

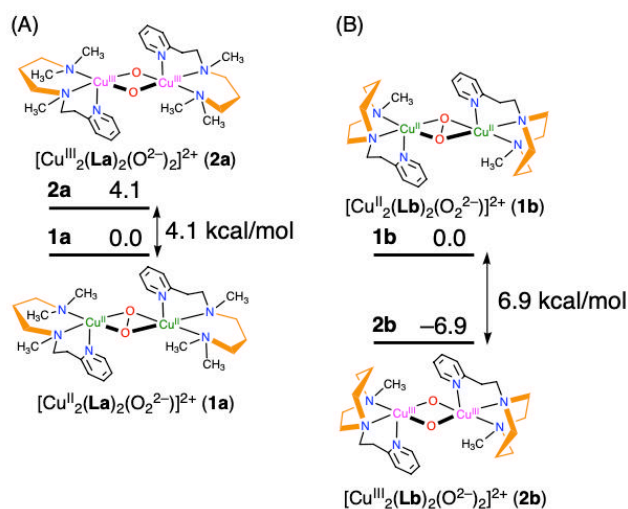


Fig. 3 Calculated energy differences between the (μ - η^2 : η^2 -peroxido)Cu^{II}Cu^{II} **1** and the bis(μ -oxido)Cu^{III}Cu^{III} complex **2** in (A) **La** and (B) **Lb** ligand systems.

We calculated harmonic frequencies at the B3LYP*-D3 level to evaluate the Raman active vibrational modes characteristic of the Cu₂O₂ core structures. Calculated Raman bands show that the Cu–Cu stretching for the breathing mode of the (μ - η^2 : η^2 -peroxido)Cu^{II}Cu^{II} core is 288 cm⁻¹ in **1a** and 274 cm⁻¹ in **1b**, as shown in Fig. 4. The calculated value for **1a** well reproduces an experimental value of 276 cm⁻¹ for **1a**.³⁶ We also confirm that these Raman bands are hardly shifted upon ¹⁸O₂-substitution. Thus, the peak positions as well as the isotope inactive bands are in good agreement with the Cu–Cu stretching bands of **1** reported by Solomon and co-workers.⁸⁰ We also obtained two kinds of Raman bands derived from the bis(μ -oxido)Cu^{III}Cu^{III} core of **2a** and **2b** at about 600 cm⁻¹. Tolman and co-workers reported that there are two types of Cu₂O₂ core vibrations, breathing and pairwise modes.⁸¹ We can also confirm these two independent vibrations including Cu–O stretching at 625 (**2a**) and 634 cm⁻¹ (**2b**) for the breathing mode and 630 (**2a**) and 598 cm⁻¹ (**2b**) for the pairwise mode. These peak shifts to 603 (**2a**) and 609 cm⁻¹ (**2b**) for the breathing mode and 609 (**2a**) and 580 cm⁻¹ (**2b**) for the pairwise mode upon ¹⁸O₂-substitution. The peak positions and the isotope shifts experimentally observed⁸¹ are consistent well with our calculations.

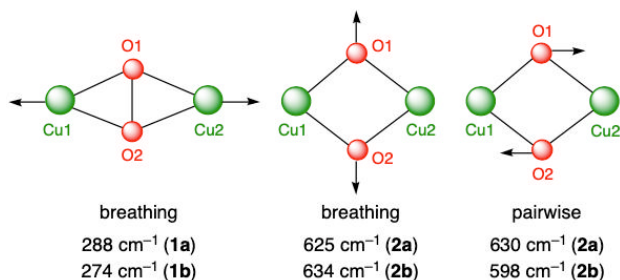


Fig. 4 Illustrations of the calculated vibrational modes and values for Cu₂O₂ cores of **1a**, **1b**, **2a** and **2b**.

Let us next look at the optimized structures of the two (μ - η^2 : η^2 -peroxido)Cu^{II}Cu^{II} complexes (**1a** and **1b**) shown in Fig. 5 to consider geometrical aspects in the stability of dicopper-dioxygen complexes. The two copper(II) ions of **1a** have a five-coordinate distorted square pyramidal structure because $\tau_5 = 0.07$ around Cu1 and 0.23 around Cu2, where τ_5 is defined as $(\beta - \alpha)/60$, β being the maximum N–Cu–O angle and α being the second maximum N–Cu–O angle. For example, $\tau_5 = 0.00$ for an ideal square pyramidal structure and $\tau_5 = 1.00$ for a trigonal-bipyramidal structure.⁸² These copper(II) ions consist of the ligands with the two nitrogen atoms N2 and N3 (N5 and N6) located in the equatorial positions and one nitrogen atom N1 (N4) located in the axial position. The peroxide moiety O1 and O2 occupies the other two equatorial positions. **1b** also has a distorted square pyramidal structure ($\tau_5 = 0.36$ and 0.20). Regarding to the Cu₂O₂ cores of **1a** and **1b**, the O1–O2 bond distances of 1.45 Å in **1a** and 1.46 Å in **1b** and the Cu1–Cu2 bond distances of 3.52 Å in **1a** and 3.42 Å in **1b** are nearly identical to the typical O–O and Cu–Cu distances of the (μ - η^2 : η^2 -peroxido)Cu^{II}Cu^{II} complexes determined by X-ray crystallography.¹ The Cu1–Cu2 distance of **1b** is shorter than that of **1a** because the structure of **1b** is more distorted than that of **1a**, where the dihedral angles Cu1–O1–O2–Cu2 are 143.1° in **1a** and 133.2° in **1b**. Large structural constrain in **1b** due to the rigidity of the cyclic diamine moiety may cause its instability.

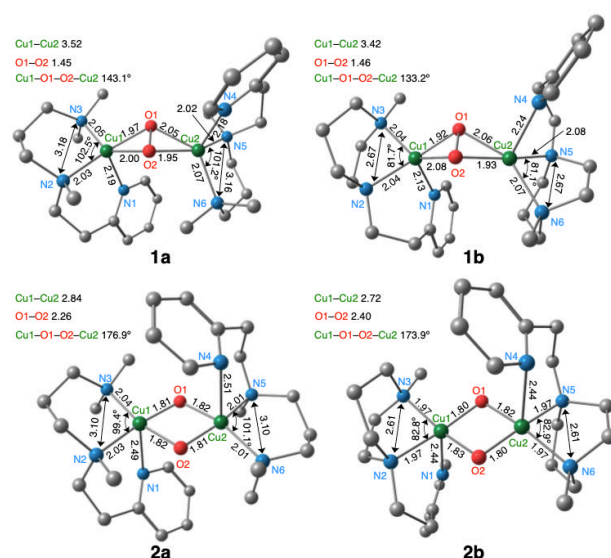


Fig. 5 Optimized structures of **1a**, **1b**, **2a** and **2b**. The units of lengths are Å. H atoms are omitted for clarity.

We further look at the optimized structures of the two bis(μ -oxido)Cu^{III}Cu^{III} complexes (**2a** and **2b**) in Fig. 5. The two copper(III) ions in the structures have five-coordinate distorted square pyramidal structures ($\tau_5 = 0.03$, 0.02 in **2a** and 0.10, 0.18 in **2b**). These copper ions consist of ligands with two nitrogen atoms N2 and N3 (N5 and N6) located in the equatorial positions and one nitrogen atom N1 (N4) located in the axial position. The two oxide ions O1 and O2 occupy the other two equatorial positions. Regarding to the Cu₂O₂ cores of **2a** and **2b**, the geometrical parameters such as the distances of Cu1–Cu2 and O1–O2 and the

dihedral angle of Cu1–O1–O2–Cu2 are similar to the reported values of the bis(μ -oxido)Cu^{III}Cu^{III} complexes determined by X-ray crystallography.¹ For **2a** and **2b**, the Cu1–Cu2 distances are shortened from 2.84 Å in **2a** to 2.72 Å in **2b** and the O1–O2 distances are elongated from 2.26 Å in **2a** to 2.40 Å in **2b** although the dihedral angles of **2a** and **2b** are comparable.

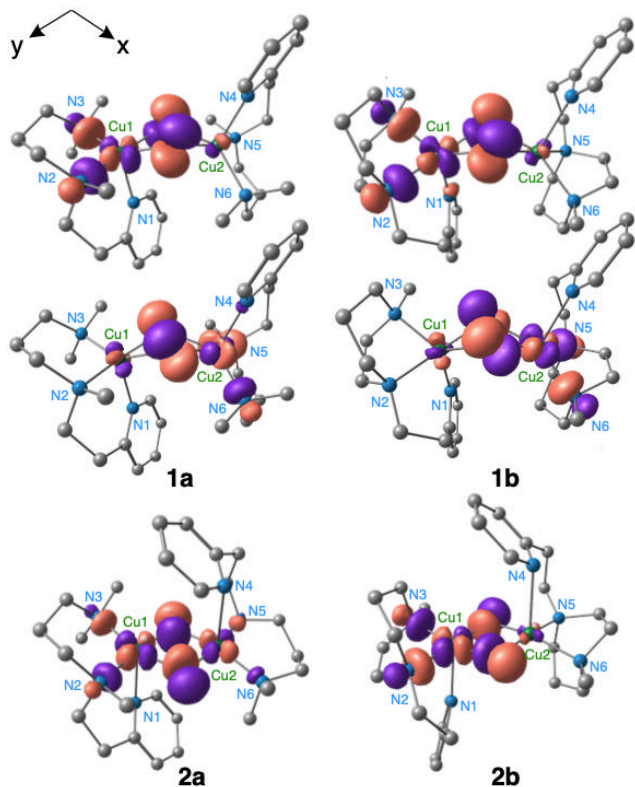


Fig. 6 Calculated SOMOs in **1a** and **1b** and LUMOs in **2a** and **2b**. H atoms are omitted for clarity.

According to the molecular orbitals in **1a**, **1b**, **2a** and **2b**, as shown in Fig. 6, the lobes of the $d_{x^2-y^2}$ orbitals of the two Cu ions are oriented to the N2–Cu1 and N3–Cu1 bonds, the x and y axes being defined in Fig. 6. The $d_{x^2-y^2}$ orbitals of the (μ - η^2 : η^2 -peroxido)Cu^{II}Cu^{II} complexes **1a** and **1b** correspond to the SOMOs (singly occupied molecular orbitals), whereas those of the bis(μ -oxido)Cu^{III}Cu^{III} complexes **2a** and **2b** correspond to the LUMOs. As the $d_{x^2-y^2}$ orbitals get higher in energy, the (μ - η^2 : η^2 -peroxido)Cu^{II}Cu^{II} complexes are destabilized because the SOMOs are likely to release the electrons, whereas the bis(μ -oxido)Cu^{III}Cu^{III} complexes are stabilized because the LUMOs are unlikely to receive the electrons. When the cone angle N2–Cu1–N3 approaches 90°, the electrostatic repulsion between the $d_{x^2-y^2}$ orbitals and the lone pair orbitals of the N2 and N3 donor atoms can be maximized according to ligand field theory. When the cone angle N2–Cu1–N3 is much larger than 90°, the (μ - η^2 : η^2 -peroxido)Cu^{II}Cu^{II} complexes can be stabilized in energy, whereas when it is close to 90°, the bis(μ -oxido)Cu^{III}Cu^{III} complexes can be stabilized. We consider that **La** can more stabilize the (μ - η^2 : η^2 -peroxido)Cu^{II}Cu^{II} complex while **Lb** can more stabilize the bis(μ -oxido)Cu^{III}Cu^{III} complex because an averaged cone angle N2–Cu1–N3 (N5–Cu2–N6) of 101.1° in **La** is larger than that of 82.1° in **Lb**, as shown in Fig. 5. In fact, the X-ray crystal structures of the (μ -

η^2 : η^2 -peroxido)Cu^{II}Cu^{II} complexes and the bis(μ -oxido)Cu^{III}Cu^{III} complexes supported by alkylamine ligands show that the average of the cone angles between the equatorial positions of the nitrogen atoms (N_{eq}) and the copper center N_{eq} –Cu– N_{eq} are 103.8° in the (μ - η^2 : η^2 -peroxido)Cu^{II}Cu^{II} complexes^{23,35} and 89° in the bis(μ -oxido)Cu^{III}Cu^{III} complexes.^{17,83–85}

Effects of the Distance between N2 and N3 in the Diamine Chelate.

To investigate whether the N2–N3 (N5–N6) distance of the diamine moiety would control the stability of the dicopper-dioxygen complexes, we calculated the relative energies [$\Delta E = E(\mathbf{2a}) - E(\mathbf{1a})$] as a function of the N2–N3 (N5–N6) distance between 2.30 Å and 3.40 Å. In **Lb**, the rigidity of the diamine chelate interferes to maintain the reasonable structure of **1b** and **2b** in the range from 2.30 Å to 3.40 Å of the N2–N3 (N5–N6) distance. Thus, we considered only the energy difference between **1a** and **2a**. As shown in Fig. 7, the change of ΔE depends on the N2–N3 (N5–N6) distance of **La**. Notably, ΔE shows a second-order hyperbolic curve with respect to the N2–N3 (N5–N6) distance of **La** ($R^2 = 0.998$). At the long N2–N3 (N5–N6) distance of 3.40 Å, **1a** is more stable than **2a** by 8.4 kcal/mol. Then, as the N2–N3 (N5–N6) distance decreases, ΔE gradually decreases to zero at the N2–N3 (N5–N6) distance of 2.69 Å (point Y in Fig. 7). In the N2–N3 (N5–N6) distance around 2.60 Å (between points X and Y), **2a** is slightly favored in energy relative to **1a** by 0.4 kcal/mol. These computed results are fully consistent with the experimental result that ligand **La** gives a mixture of **1a** (major product) and **2a** (minor product).³⁶ Fig. 7 indicates that the formation of the bis(μ -oxido)Cu^{III}Cu^{III} complexes is made when the N2–N3 (N5–N6) distance is in between 2.43 Å and 2.69 Å (between X and Y). In fact, since the N2–N3 (N5–N6) distance is 2.61 Å in **2b**, as shown in Fig. 5, **2b** is energetically more stable than **1b**.

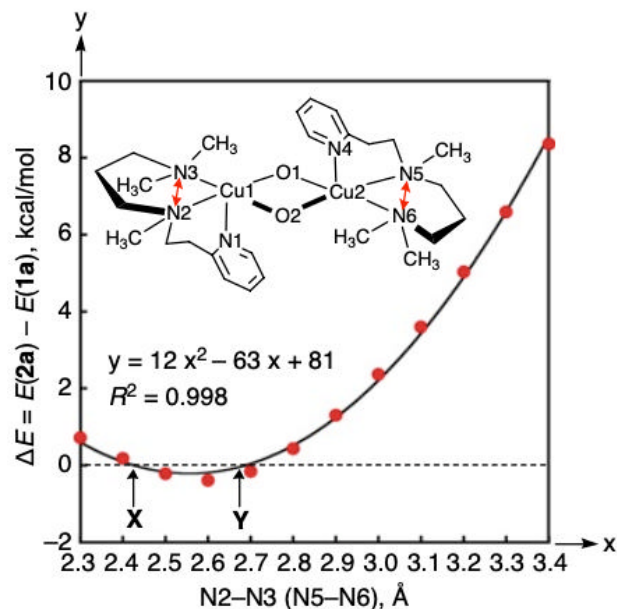


Fig. 7 Plots of energy difference, $\Delta E = E(\mathbf{2a}) - E(\mathbf{1a})$ as a function of the N2–N3 (N5–N6) distance in **La**. A dotted line stands for the equal of the energies of **1a** and **2a**. ΔE is zero at the N2–N3 (N5–N6) distances of 2.43 (point X) and 2.69 (point Y).

We next take a look at the molecular orbitals of **1a** and **2a** along the N2–N3 (N5–N6) distance to understand the reason why O₂ is more activated when the chelate diamine moiety is shrunk. The Cu₂O₂ core involves the three key orbitals formed from the mixture of the σ^* orbital of the O–O moiety and the d_{Ax2-y2} and d_{Bx2-y2} orbitals of the Cu ions, as shown in Fig. 8(A) and 8(B). Let us first consider the electronic configuration of the two electrons in the three orbitals. In the $(\mu\text{-}\eta^2\text{-}\eta^2\text{-peroxido})\text{Cu}^{\text{II}}\text{Cu}^{\text{II}}$ complexes, the σ^* orbital of O₂²⁻ lies far above the d_{x2-y2} orbitals,⁴⁹ so that the σ^* orbital of **1a** would not interact with the d_{x2-y2} orbitals of the Cu^{II} ions, the x and y axes being defined in Fig. 8. Therefore, one can consider that the triplet or open-shell singlet state should be the ground state of **1a**, as shown in Fig. 8(A).

Once the O–O bond of the $(\mu\text{-}\eta^2\text{-}\eta^2\text{-peroxido})\text{Cu}^{\text{II}}\text{Cu}^{\text{II}}$ complex is cleaved, the σ^* orbital of the dioxygen moiety goes down to lie below the d_{x2-y2} orbitals of the Cu ions.⁴⁹ Consequently, the two electrons accommodated in the two d_{x2-y2} orbitals would transfer to the σ^* orbital with a reconstruction of its bonding nature. Therefore, the HOMO of the bis(μ -oxido)Cu^{III}Cu^{III} complex mainly consists of the $d_{x2-y2} + \sigma^*$ orbital while the LUMOs consist of the $d_{Ax2-y2} - \sigma^*$ and $d_{Bx2-y2} - \sigma^*$ orbitals, where + and – show bonding and antibonding interactions, respectively. This orbital analysis tells us that the energy levels of the σ^* orbital of the dioxygen moiety and the two d_{x2-y2} orbitals can control the spin state and the interconversion between **1a** and **2a**.

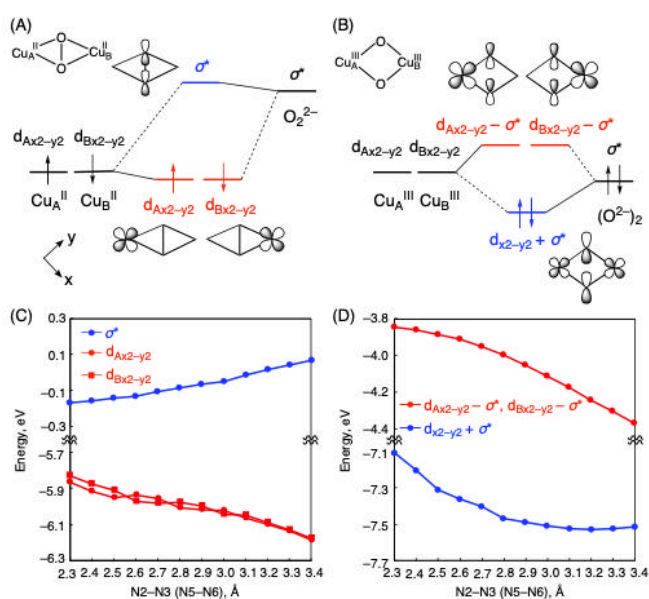


Fig. 8 Schematic representation of the key molecular orbitals in the conversion from (A) **1a** to (B) **2a**. Walsh diagrams of (C) σ^* , d_{Ax2-y2} and d_{Bx2-y2} orbitals along the distance of the diamine framework N2–N3 (N5–N6) in **1a** and (D) $d_{Ax2-y2} - \sigma^*$, $d_{Bx2-y2} - \sigma^*$ and $d_{x2-y2} + \sigma^*$ orbitals along the distance of the diamine framework N2–N3 (N5–N6) in **2a**. $d_{Ax2-y2} - \sigma^*$ and $d_{Bx2-y2} - \sigma^*$ orbitals are degenerate in **2a**.

The energies of the molecular orbitals are significantly changed as a function of the N2–N3 (N5–N6) distance in **1a**. As the N2–N3 (N5–N6) distance is shortened, the energies of the d_{Ax2-y2} and d_{Bx2-y2} orbitals go up, as shown in Fig. 8(C). The lobes of the d_{x2-y2} orbitals of the Cu^{II} ions are oriented well to the N2–Cu1 (N5–Cu2) and N3–Cu1 (N6–Cu2) bonds, as shown in Fig. 6. Since the

cone angle N2–Cu1–N3 (N5–Cu2–N6) is reduced along with the decrease of the N2–N3 (N5–N6) distance, the overlap between the d_{x2-y2} orbitals of the Cu^{II} ions and the lone pair orbitals of the N2 and N3 (N5 and N6) atoms increases, resulting in that the bonding orbital consisting of the d_{Ax2-y2} and d_{Bx2-y2} orbitals of the Cu^{II} ions and the lone pair orbitals of the N2 and N3 (N5 and N6) atoms goes down in energy while the antibonding orbital consisting of them goes up (Fig. S3 of the ESI). This antibonding orbital is the SOMO corresponding to the d_{Ax2-y2} (d_{Bx2-y2}) orbital in Fig. 8(A). Therefore, when the N2–N3 (N5–N6) distance decreases, the energy of the d_{Ax2-y2} (d_{Bx2-y2}) orbitals goes up, leading to decrease the energy gap between the σ^* orbital and the d_{Ax2-y2} (d_{Bx2-y2}) orbital (Figs. 8(C) and S4 of the ESI). Since the small energy gap enhances the contribution of the σ^* orbital in the SOMOs of **1a**, the injection of more electrons into the σ^* orbital occurs concomitant with the elongation of the O1–O2 bond distance. Calculated bond order of the O1–O2 bond decreases as the N2–N3 (N5–N6) distance decreases in **1a**, as shown in Figs. S5 and S6 of the ESI. In fact, the electron injection into the σ^* orbital is efficient enough to elongate the O1–O2 bond distance in **1a**.^{35,50,86}

As the N2–N3 (N5–N6) distance decreases, the $d_{Ax2-y2} - \sigma^*$ and $d_{Bx2-y2} - \sigma^*$ orbitals in **2a** are destabilized, as seen in Fig. 8(D). In contrast, the energy of the $d_{x2-y2} + \sigma^*$ orbital remains unchanged in between 3.40 Å and 2.80 Å while there is an increase in between 2.80 Å and 2.30 Å. Calculated energy gaps between the $d_{Ax2-y2} - \sigma^*$ and $d_{Bx2-y2} - \sigma^*$ orbitals and the $d_{x2-y2} + \sigma^*$ orbital increase from 3.14 eV at 3.40 Å to 3.47 eV at 2.80 Å. They are nearly constant in the range from 3.47 eV at 2.80 Å to 3.45 eV at 2.60 Å. They decrease from 3.45 eV at 2.60 Å to 3.26 eV at 2.30 Å, as shown in Fig. S7 of the ESI. Thus, our MO analyses indicate that the range between 2.80 Å and 2.60 Å of the N2–N3 (N5–N6) distance is suited for the stabilization of the bis(μ -oxido)Cu^{III}Cu^{III} complex if we ignore the distortion energy from the ligands. Actually, it is small enough.

Conclusions

In summary, we have carried out a computational study on the $(\mu\text{-}\eta^2\text{-}\eta^2\text{-peroxido})\text{Cu}^{\text{II}}\text{Cu}^{\text{II}}$ complexes **1** and the bis(μ -oxido)Cu^{III}Cu^{III} complexes **2** having N₃-tridentate ligands **La** and **Lb** using the B3LYP*-D3 functional. The calculated Cu–Cu stretching vibrational frequencies of the $(\mu\text{-}\eta^2\text{-}\eta^2\text{-peroxido})\text{Cu}^{\text{II}}\text{Cu}^{\text{II}}$ complexes **1a** and **1b** are 288 and 274 cm⁻¹, respectively, which are in good agreement with the experimental resonance Raman bands.³⁶ For the bis(μ -oxido)Cu^{III}Cu^{III} complexes **2a** and **2b**, there are two different types of vibrational modes, which are breathing and pairwise modes. The peak positions as well as the isotope shifts upon ¹⁸O₂-substitution of the Cu–O stretching in **2a** and **2b** are consistent with those of the reported bis(μ -oxido)Cu^{III}Cu^{III} complexes. The B3LYP*-D3 functional was found to be effective to evaluate not only the vibrational frequencies but also the relative energies of **1** and **2**. [Cu^{II}₂(**La**)₂(O₂²⁻)₂]²⁺ (**1a**) is 4.1 kcal/mol more stable than [Cu^{III}₂(**La**)₂(O₂²⁻)₂]²⁺ (**2a**), whereas [Cu^{III}₂(**Lb**)₂(O₂²⁻)₂]²⁺ (**2b**) is 6.9 kcal/mol more stable than [Cu^{II}₂(**Lb**)₂(O₂²⁻)₂]²⁺ (**1b**). These results agree well with the

experimental results that **La** provides **1a** as a major product, whereas **Lb** analogue gives **2b** predominantly.³⁶

To investigate the perturbational effects from the ligand frameworks on the stability of the Cu₂O₂ complexes, we calculated the potential energies of **1a** and **2a** at the distance of N2–N3 (N5–N6) of **La** from 2.30 Å to 3.40 Å. Clearly, the relative energy between **1a** and **2a** depends on the N2–N3 (N5–N6) distance of **La**, showing a second-order hyperbolic curve with respect to the N2–N3 (N5–N6) distance of **La**, as shown in Fig. 7. At the N2–N3 (N5–N6) distance of 3.40 Å, **1a** is 8.4 kcal/mol more stable than **2a**. As the diamine moiety is shrunk, the relative energy between **1a** and **2a** decreases to zero at the N2–N3 (N5–N6) distance of 2.69 Å. The formation of the bis(μ -oxido)Cu^{II}Cu^{III} complexes is made when the distance between the two N atoms located in the equatorial positions is in between 2.43 Å and 2.69 Å.

To clarify the reason why O₂ is more activated when the chelate diamine moiety is shrunk, we analyzed molecular orbitals of **1** and **2** by considering the electronic configuration of two electrons in the two 3d orbitals of the Cu^{II} ions and the σ^* orbital of the O–O moiety. For the (μ - η^2 : η^2 -peroxido)Cu^{II}Cu^{II} complexes, the σ^* orbital is higher in energy than the d_{x₂-y₂} orbitals of the Cu^{II} ions, resulting in that the σ^* orbital of **1a** little interacts with the d_{x₂-y₂} orbitals of the Cu^{II} ions. When the (μ - η^2 : η^2 -peroxido)Cu^{II}Cu^{II} complexes covert into the bis(μ -oxido)Cu^{II}Cu^{III} complexes, the σ^* orbital is lower in energy than the d_{x₂-y₂} orbitals of the Cu^{III} ions. Our MO analyses suggest that the N2–N3 distance can finely tune the interactions between the lone pair orbitals of the N2 and N3 atoms and the d_{x₂-y₂} orbitals of the Cu ions, demonstrating that the interactions between the d_{x₂-y₂} orbitals of the Cu ions and the σ^* orbital of the O–O bond can control the equilibrium of the (μ - η^2 : η^2 -peroxido)Cu^{II}Cu^{II} complex and the bis(μ -oxido)Cu^{II}Cu^{III} complex. These results provide new insights into the design of dicopper complexes and their catalytic activity.

Conflicts of interest

There are no conflicts to declare.

Acknowledgements

K.Y. acknowledges KAKENHI Grant numbers JP15K13710 and JP17H03117 from Japan Society for the Promotion of Science (JSPS) and the Ministry of Education, Culture, Sports, Science and Technology of Japan (MEXT), the MEXT Projects of “Integrated Research Consortium on Chemical Sciences”, “Cooperative Research Program of Network Joint Research Center for Materials and Devices”, “Elements Strategy Initiative to Form Core Research Center”, JST-CREST JPMJCR15P5 and JST-Mirai JPMJMI18A2. The computational study was mainly carried out using the computer facilities at Research Institute for Information Technology, Kyushu University.

References

- 1 L. M. Mirica, X. Ottenwaelder and T. D. P. Stack, *Chem. Rev.*, 2004, **104**, 1013–1045.
- 2 E. A. Lewis and W. B. Tolman, *Chem. Rev.*, 2004, **104**, 1047–1076.
- 3 L. Q. Hatcher and K. D. Karlin, *J. Biol. Inorg. Chem.*, 2004, **9**, 669–683.
- 4 S. Itoh and S. Fukuzumi, *Acc. Chem. Res.*, 2007, **40**, 592–600.
- 5 S. Itoh, *Copper-Oxygen Chemistry*; K. D. Karlin and S. Itoh, Eds.; John Wiley & Sons, Inc.: Hoboken, 2011, **4**, 225–282.
- 6 E. I. Solomon, D. E. Heppner, E. M. Johnston, J. W. Ginsbach, J. Cirera, M. Qayyum, M. T. Kieber-Emmons, C. H. Kjaergaard, R. G. Hadt and L. Tian, *Chem. Rev.*, 2014, **114**, 3659–3853.
- 7 C. E. Elwell, N. L. Gagnon, B. D. Neisen, D. Dhar, A. D. Spaeth, G. M. Yee and W. B. Tolman, *Chem. Rev.*, 2017, **117**, 2059–2107.
- 8 E. I. Solomon, U. M. Sundaram and T. E. Machonkin, *Chem. Rev.*, 1996, **96**, 2563–2605.
- 9 K. A. Magnus, H. Ton-That and J. E. Carpenter, *Chem. Rev.*, 1994, **94**, 727–735.
- 10 Y. Matoba, T. Kumagai, A. Yamamoto, H. Yoshitsu and M. Sugiyama, *J. Biol. Chem.*, 2006, **281**, 8981–8990.
- 11 C. Gerdemann, C. Eicken and B. Krebs, *Acc. Chem. Res.*, 2002, **35**, 183–191.
- 12 N. Kitajima, K. Fujisawa and Y. Moro-oka, *J. Am. Chem. Soc.*, 1989, **111**, 8976–8978.
- 13 N. Kitajima, K. Fujisawa, C. Fujimoto, Y. Moro-oka, S. Hashimoto, T. Kitagawa, K. Toriumi, K. Tatsumi and A. Nakamura, *J. Am. Chem. Soc.*, 1992, **114**, 1277–1291.
- 14 N. Kitajima and Y. Moro-oka, *Chem. Rev.*, 1994, **94**, 737–757.
- 15 S. Mahapatra, J. A. Halfen, E. C. Wilkinson, G. Pan, C. J. Cramer, L. Que and W. B. Tolman, *J. Am. Chem. Soc.*, 1995, **117**, 8865–8866.
- 16 J. A. Halfen, S. Mahapatra, E. C. Wilkinson, S. Kaderli, V. G. Young, L. Que, A. D. Zuberbühler and W. B. Tolman, *Science*, 1996, **271**, 1397–1400.
- 17 S. Mahapatra, J. A. Halfen, E. C. Wilkinson, G. Pan, X. Wang, V. G. Young, C. J. Cramer, L. Que and W. B. Tolman, *J. Am. Chem. Soc.*, 1996, **118**, 11555–11574.
- 18 L. M. Mirica, M. Vance, D. J. Rudd, B. Hedman, K. O. Hodgson, E. I. Solomon and T. D. P. Stack, *Science*, 2005, **308**, 1890–1892.
- 19 C. Citek, S. Herres-Pawlis and T. D. P. Stack, *Acc. Chem. Res.*, 2015, **48**, 2424–2433.
- 20 P. L. Holland and W. B. Tolman, *Coord. Chem. Rev.*, 1999, **190–192**, 855–869.
- 21 K. D. Karlin, M. S. Haka, R. W. Cruse, G. J. Meyer, A. Farooq, Y. Gultneh, J. C. Hayes and J. Zubieta, *J. Am. Chem. Soc.*, 1988, **110**, 1196–1207.
- 22 V. Mahadevan, M. J. Henson, E. I. Solomon and T. D. P. Stack, *J. Am. Chem. Soc.*, 2000, **122**, 110249–10250.
- 23 B. M. T. Lam, J. A. Halfen, V. C. Young, J. R. Hagadorn, P. L. Holland, A. Lledós, L. Cucurull-Sánchez, J. J. Novoa, S. Alvarez and W. B. Tolman, *Inorg. Chem.*, 2000, **39**, 4059–4072.
- 24 S. Itoh, H. Kumei, M. Taki, S. Nagatomo, T. Kitagawa and S. Fukuzumi, *J. Am. Chem. Soc.*, 2001, **123**, 6708–6709.
- 25 H.-C. Liang, C. X. Zhang, M. J. Henson, R. D. Sommer, K. R. Hatwell, S. Kaderli, A. D. Zuberbühler, A. L. Rheingold, E. I. Solomon and K. D. Karlin, *J. Am. Chem. Soc.*, 2002, **124**, 4170–4171.
- 26 T. Osako, Y. Ueno, Y. Tachi and S. Itoh, *Inorg. Chem.*, 2003, **42**, 8087–8097.
- 27 C. X. Zhang, H.-C. Liang, E.-i. Kim, J. Shearer, M. E. Helton, E. Kim, S. Kaderli, C. D. Incarvito, A. D. Zuberbühler, A. L. Rheingold and K. D. Karlin, *J. Am. Chem. Soc.*, 2003, **125**, 634–635.
- 28 M. J. Henson, M. A. Vance, C. X. Zhang, H.-C. Liang, K. D. Karlin and E. I. Solomon, *J. Am. Chem. Soc.*, 2003, **125**, 5186–5192.

- 29 T. Osako, S. Terada, T. Tosha, S. Nagatomo, H. Furutachi, S. Fujinami, T. Kitagawa, M. Suzuki and S. Itoh, *Dalton Trans.*, 2005, 3514–3521.
- 30 S. Itoh and Y. Tachi, *Dalton Trans.*, 2006, 4531–4538.
- 31 A. Kunishita, T. Osako, Y. Tachi, J. Teraoka and S. Itoh, *Bull. Chem. Soc. Jpn.*, 2006, **79**, 1729–1741.
- 32 L. Q. Hatcher, M. A. Vance, A. A. Narducci Sarjeant, E. I. Solomon and K. D. Karlin, *Inorg. Chem.*, 2006, **45**, 3004–3013.
- 33 O. Sander, C. Näther and F. Tuczek, *Z. Anorg. Allg. Chem.*, 2009, **635**, 1123–1133.
- 34 G. Y. Park, Y. Lee, D.-H. Lee, J. S. Woertink, A. A. Narducci Sarjeant, E. I. Solomon and K. D. Karlin, *Chem. Commun.*, 2010, **46**, 91–93.
- 35 G. Y. Park, M. F. Qayyum, J. Woertink, K. O. Hodgson, B. Hedman, A. A. Narducci Sarjeant, E. I. Solomon and K. D. Karlin, *J. Am. Chem. Soc.*, 2012, **134**, 8513–8524.
- 36 T. Abe, Y. Morimoto, T. Tano, K. Mieda, H. Sugimoto, N. Fujieda, T. Ogura and S. Itoh, *Inorg. Chem.*, 2014, **53**, 8786–8794.
- 37 S. Itoh, *Acc. Chem. Res.*, 2015, **48**, 2066–2074.
- 38 J. Cahoy, P. L. Holland and W. B. Tolman, *Inorg. Chem.*, 1999, **38**, 2161–2168.
- 39 T. D. P. Stack, *Dalton Trans.*, 2003, 1881–1889.
- 40 H.-C. Liang, M. J. Henson, L. Q. Hatcher, M. A. Vance, C. X. Zhang, D. Lahti, S. Kaderli, R. D. Sommer, A. L. Rheingold, A. D. Zuberbühler, E. I. Solomon and K. D. Karlin, *Inorg. Chem.*, 2004, **43**, 4115–4117.
- 41 X. Ottenwaelder, D. J. Rudd, M. C. Corbett, K. O. Hodgson, B. Hedman and T. D. P. Stack, *J. Am. Chem. Soc.*, 2006, **128**, 9268–9269.
- 42 A. K. Gupta and W. B. Tolman, *Inorg. Chem.*, 2010, **49**, 3531–3539.
- 43 J. Maddaluno and C. Giessner-Prettre, *Inorg. Chem.*, 1991, **30**, 3439–3445.
- 44 E. I. Solomon, M. J. Baldwin and M. D. Lowery, *Chem. Rev.*, 1992, **92**, 521–542.
- 45 E. I. Solomon and M. D. Lowery, *Science*, 1993, **259**, 1575–1581.
- 46 E. I. Solomon, F. Tuczek, D. E. Root and C. A. Brown, *Chem. Rev.*, 1994, **94**, 827–856.
- 47 I. Bytheway and M. B. Hall, *Chem. Rev.*, 1994, **94**, 639–658.
- 48 B. J. Gherman and C. J. Cramer, *Coord. Chem. Rev.*, 2009, **253**, 723–753.
- 49 K. Yoshizawa, T. Ohta and T. Yamabe, *Bull. Chem. Soc. Jpn.*, 1997, **70**, 1911–1917.
- 50 P. K. Ross and E. I. Solomon, *J. Am. Chem. Soc.*, 1991, **113**, 3246–3259.
- 51 F. Bernardi, A. Bottoni, R. Casadio, P. Fariselli and A. Rigo, *Inorg. Chem.*, 1996, **35**, 5207–5212.
- 52 C. J. Cramer, B. A. Smith and W. B. Tolman, *J. Am. Chem. Soc.*, 1996, **118**, 11283–11287.
- 53 O. Eisenstein, H. Getlicherman, C. Giessner-Prettre and J. Maddaluno, *Inorg. Chem.*, 1997, **36**, 3455–3460.
- 54 X.-Y. Liu, A. A. Palacios, J. J. Novoa and S. Alvarez, *Inorg. Chem.*, 1998, **37**, 1202–1212.
- 55 M. Flock and K. Pierloot, *J. Phys. Chem. A*, 1999, **103**, 95–102.
- 56 G. S. Nikolov, H. Mikosch and G. Bauer, *J. Mol. Struct. (THEOCHEM)*, 2000, **499**, 35–50.
- 57 C. J. Cramer, M. Wloch, P. Piecuch, C. Puzzarini and L. Gagliardi, *J. Phys. Chem. A*, 2006, **110**, 1991–2004.
- 58 C. J. Cramer, M. Wloch, P. Piecuch, C. Puzzarini and L. Gagliardi, *J. Phys. Chem. A*, 2006, **110**, 11557–11568.
- 59 A. Bérces, *Inorg. Chem.*, 1997, **36**, 4831–4837.
- 60 A. Bérces, *Int. J. Quant. Chem.*, 1997, **65**, 1077–1086.
- 61 M. J. Henson, P. Mukherjee, D. E. Root, T. D. P. Stack and E. I. Solomon, *J. Am. Chem. Soc.*, 1999, **121**, 10332–10345.
- 62 P. E. M. Siegbahn and M. Wirstam, *J. Am. Chem. Soc.*, 2001, **123**, 11819–11820.
- 63 P. E. M. Siegbahn, *J. Biol. Inorg. Chem.*, 2003, **8**, 577–585.
- 64 C. J. Cramer, C. R. Kinsinger and Y. Pak, *J. Mol. Struct. (THEOCHEM)*, 2003, **632**, 111–120.
- 65 M. F. Rode and H.-J. Werner, *Theor. Chem. Acc.*, 2005, **114**, 309–317.
- 66 J. L. Lewin, D. E. Heppner and C. J. Cramer, *J. Biol. Inorg. Chem.*, 2007, **12**, 1221–1234.
- 67 D. G. Liakos and F. Neese, *J. Chem. Theory Comput.* 2011, **7**, 1511–1523; F. Neese, D. G. Liakos and S. Ye, *J. Biol. Inorg. Chem.*, 2011, **16**, 821–829.
- 68 A. Poater and L. Cavallo, *Theor. Chem. Acc.*, 2013, **132**, 1336–1349.
- 69 M. Rohrmüller, S. Herres-Pawlis, M. Witte and W. G. Schmidt, *J. Comput. Chem.*, 2013, **34**, 1035–1045.
- 70 M. Rohrmüller, A. Hoffmann, C. Thierfelder, S. Herres-Pawlis and W. G. Schmidt, *J. Comput. Chem.*, 2015, **36**, 1672–1685.
- 71 M. Witte and S. Herres-Pawlis, *Phys. Chem. Chem. Phys.*, 2017, **19**, 26880–26889.
- 72 A. D. Becke, *Phys. Rev. A*, 1988, **38**, 3098–3100; C. Lee, W. Yang and R. G. Parr, *Phys. Rev. B*, 1988, **37**, 785–789; A. D. Becke, *J. Chem. Phys.*, 1993, **98**, 5648–5652.
- 73 M. Reiher, O. Salomon and B. A. Hess, *Theor. Chem. Acc.*, 2001, **107**, 48–55; O. Salomon, M. Reiher and B. A. Hess, *J. Chem. Phys.*, 2002, **117**, 4729–4737.
- 74 M. J. Frisch, G. W. Trucks, H. B. Schlegel, G. E. Scuseria, M. A. Robb, J. R. Cheeseman, G. Scalmani, V. Barone, G. A. Petersson, H. Nakatsuji, X. Li, M. Caricato, A. V. Marenich, J. Bloino, B. G. Janesko, R. Gomperts, B. Mennucci, H. P. Hratchian, J. V. Ortiz, A. F. Izmaylov, J. L. Sonnenberg, D. Williams-Young, F. Ding, F. Lipparini, F. Egidi, J. Goings, B. Peng, A. Petrone, T. Henderson, D. Ranasinghe, V. G. Zakrzewski, J. Gao, N. Rega, G. Zheng, W. Liang, M. Hada, M. Ehara, K. Toyota, R. Fukuda, J. Hasegawa, M. Ishida, T. Nakajima, Y. Honda, O. Kitao, H. Nakai, T. Vreven, K. Throssell, J. A. Montgomery, Jr., J. E. Peralta, F. Ogliaro, M. J. Bearpark, J. J. Heyd, E. N. Brothers, K. N. Kudin, V. N. Staroverov, T. A. Keith, R. Kobayashi, J. Normand, K. Raghavachari, A. P. Rendell, J. C. Burant, S. S. Iyengar, J. Tomasi, M. Cossi, J. M. Millam, M. Klene, C. Adamo, R. Cammi, J. W. Ochterski, R. L. Martin, K. Morokuma, O. Farkas, J. B. Foresman and D. J. Fox, Gaussian 16, Revision A. 03; Gaussian, Inc.: Wallingford, CT, 2016.
- 75 A. J. H. Wachters, *J. Chem. Phys.*, 1970, **52**, 1033–1036; P. J. Hay, *J. Chem. Phys.*, 1977, **66**, 4377–4384; K. Raghavachari and G. W. Trucks, *J. Chem. Phys.*, 1989, **91**, 1062–1065.
- 76 T. H. Dunning and P. J. Hay, *In Modern Theoretical Chemistry; H. F. Schaefer, III, Ed.; Plenum: New York*, 1976, **3**, 1–27.
- 77 T. Schwabe and S. Grimme, *Phys. Chem. Chem. Phys.*, 2007, **9**, 3397–3406; S. Grimme, J. Antony, S. Ehrlich and H. Krieg, *J. Chem. Phys.*, 2010, **132**, 154104–154119.
- 78 M. R. A. Blomberg and P. E. M. Siegbahn, *Biochim. Biophys. Acta, Bioenerg.*, 2015, **1847**, 364–376; P. E. M. Siegbahn and M. R. A. Blomberg, *Front. Chem.*, 2018, **6**, 644.
- 79 J. Tomasi, B. Mennucci and R. Cammi, *Chem. Rev.*, 2005, **105**, 2999–3093.
- 80 M. J. Henson, V. Mahadevan, T. D. P. Stack and E. I. Solomon, *Inorg. Chem.*, 2001, **40**, 5068–5069.
- 81 P. L. Holland, C. J. Cramer, E. C. Wilkinson, S. Mahapatra, K. R. Rodgers, S. Itoh, M. Taki, S. Fukuzumi, L. Que and W. B. Tolman, *J. Am. Chem. Soc.*, 2000, **122**, 792–802.
- 82 A. W. Addison, T. N. Rao, J. Reedijk, J. Rijn and G. C. Verschoor, *J. Chem. Soc., Dalton Trans.*, 1984, 1349–1356; L. Yang, D. R. Powell and R. P. Houser, *Dalton Trans.*, 2007, 955–964.
- 83 V. Mahadevan, Z. Hou, A. P. Cole, D. E. Root, T. K. Lal, E. I. Solomon and T. D. P. Stack, *J. Am. Chem. Soc.*, 1997, **119**, 11996–11997.
- 84 S. Mahapatra, V. G. Young, S. Kaderli, A. D. Zuberbühler and W. B. Tolman, *Angew. Chem., Int. Ed.*, 1997, **36**, 130–133.

ARTICLE

Journal Name

- 85 A. P. Cole, V. Mahadevan, L. M. Mirica, X. Ottenwaelder, T. D. P. Stack, *Inorg. Chem.*, 2005, **44**, 7345–7364.
- 86 P. Chen, K. Fujisawa, M. E. Helton, K. D. Karlin and E. I. Solomon, *J. Am. Chem. Soc.*, 2003, **125**, 6394–6408.

